Journal of Materials and Environmental Sciences
ISSN : 2028-2508

Copyright © 2017,
University of Mohammed Premier
Oujda Morocco

JMES, 2017 Volume 8, Issue 4, Page 1448-1459

http://www.imaterenvironsci.com/

Adsorption Studies with a New Biosorbent *Ensis siliqua* Shell Powder for Removal Two Textile Dyes from Aqueous Solution

Imane Hachoumi[1], Imane El Ouahabi[1], Rachid Slimani[1], Benoît Cagnon[2], Mohammadine El Haddad[3], Said El Antri[1], Said Lazar[1*]

[1]*Laboratory of Biochemistry, Food & Environment, UARC 36, University of Hassan II-Casablanca, Mohammedia, Morocco*
[2]*Interfaces, Containment, Materials & Nanostructures (ICMN-UMR 7374). CNRS - University of Orleans, France*
[3]*Team of Analytical Chemistry & Environment, University of Cadi Ayyad, Safi, Morocco*

Received 28 Nov 2016,
Revised 13 Jan 2017,
Accepted 18 Jan 2017

Keywords

- ✓ Direct Blue 71;
- ✓ Disperse Red 60;
- ✓ Calcined Ensis siliqua shells;
- ✓ Biosorption;
- ✓ Kinetics ;
- ✓ Isotherms ;
- ✓ Thermodynamics

Said Lazar
lazar_said@yahoo.com

ABSTRACT

The presence of dyes in effluents is a long-standing problem and can cause considerable damage to the ecosystem of the receiving surface water resources. The development of efficient, relatively inexpensive and environmentally friendly natural adsorbent *Ensis siliqua* shells was applied for the removal of two textile dyes, Direct Blue 71 (DB_{71}) and Disperse Red 60 (DR_{60}), from aqueous solutions. The influence of solution pH, adsorbent dose, contact time, temperature and initial dye concentration on the adsorption process was studied. Adsorption isotherm data were analyzed using the Langmuir, Temkin, Freundlich and Dubinin–Radushkevich models. The Freundlich isotherm was found to represent the measured sorption data well. Kinetics of the adsorption reaction followed the pseudo second-order kinetic model. The maximum adsorption capacities at 25°C were 332.22 $mg.g^{-1}$ and 384.29 $mg.g^{-1}$ for DR_{60} and DB_{71} respectively. Various thermodynamic parameters such as ΔG^o, ΔH^o and ΔS^o were calculated, indicating that this system was a spontaneous and endothermic process.

1. Introduction

The textile industry discharges a large volume of polluted effluents into the environment compared to other industries such as food processing, paper, cosmetics and carpet industries. These effluents have complex chemical structures that make them inert and difficult to biodegrade when discharged into waste streams [1]. The presence of dyes in effluents causes considerable damage to the ecosystem of the receiving surface water, pollutes the groundwater resources [2], and can be highly toxic for human health.

A large number of methods are traditionally used for color removal: chemical oxidation [3], coagulation [4], electrochemical oxidation [5], coagulation/flocculation [6], advanced oxidation processes [7], ozonation [8], membrane filtration [9], electroflotation [10], electrokinetic coagulation [11], electrochemical destruction [12], ion exchange [13], irradiation [14], precipitation [15] and biological treatment [16]. All these methods have significant disadvantages such as incomplete ion removal, high-energy requirements and production of toxic sludge or other waste products that require further disposal [17]. Compared to the above-mentioned methods, adsorption is considered superior to other techniques because of its low cost, simplicity of design, availability and ability to treat dyes in more concentrated form [18].

There is therefore a growing interest in searching for alternative materials, which are relatively cost-effective and at the same time have high adsorption efficiency [19]. The following are examples of waste materials used in dye removal: wheat shells [20], calcined mussel shells [1], calcined eggshells [19], animal bone meal [21], limpet shells [22], almond shells [23], Opuntia ficus-indica fruit waste [24], soy meal hull [25], and orange peels [26].

The goal of the present research is to develop a new potential biosorbent to remove textile dyes from aqueous solution by adsorption method using *Ensis siliqua* shell waste as a novel and eco-friendly biosorbent which is a

very cheap and readily available material in most countries. The effect of several parameters such as pH, adsorbent dosage, contact time, temperature and initial dye concentration on the biosorption efficiency of Direct Blue 71 (DB_{71}) and Disperse Red 60 (DR_{60}) dyes was evaluated. The biosorption behavior was analyzed using the Langmuir, Freundlich, Temkin and Dubinin-Radushkevich adsorption isotherms. The experimental data of adsorption kinetics were analyzed using the pseudo-first and pseudo-second order kinetic models and the thermodynamics of this process were also studied.

2. Experimental details

2.1. *Preparation of adsorbent*

The pod razor shells (*Ensis siliqua*) were collected from a fisherman in a local market near Mohammedia in Morocco. The collected materials were washed several times with distilled water to remove all dirt particles. They were then oven dried at 65°C for 24 h.

The *Ensis siliqua* shells were crushed, powdered to small grains and then calcined at 800°C for 2 h. The residue was washed with distilled water three times and dried at 80°C for 24 h then finely chopped and ground into small particles, milled in an agate mortar, washed with distilled water, and dried overnight at 105°C. The adsorbent was calcined at 400°C and then maintained at this temperature for 3 h.

The resulting material was stored in a glass bottle and the calcined *Ensis siliqua* shells obtained were denominated (CESS).

2.2 *Reagents and solutions*

Two dyes were used in this study. Disperse Red dye 60 (DR_{60}) and Direct Blue dye 71 (DB_{71}) were obtained from a local textile factory in Casablanca (Morocco) and were used without further purification. The chemical structures of these dyes are shown in Figure 1. Distilled water was employed throughout as solvent. For each dye type, the optimum absorbance wavelength was found to be 579 nm for DR_{60} and 575 nm for DB_{71}.

The initial pH of the solution was adjusted by adding a small amount of HCl or NaOH (1M).

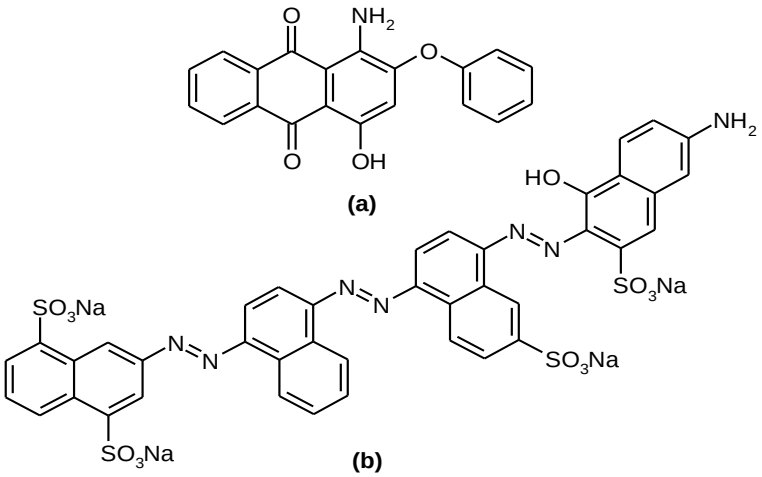

Figure 1: Chemical structures of textile dyes: (a) Disperse Red 60 (DR_{60}); (b) Direct Blue 71 (DB_{71})

2.3 *Batch adsorption experiments*

A stock solution of each dye (DR_{60} and DB_{71}) was prepared by dissolving 25 mg of dye in 1000 mL of double distilled water to prepare the desired concentrations of dye solutions. The experimental solutions of different concentrations ranging from 25 to 50 $mg.L^{-1}$ were made by further dilutions.

Adsorption studies for the evaluation of *Ensis siliqua* shells (CESS) for the removal of DR_{60} and DB_{71} dyes from aqueous solutions were carried out in triplicate using a batch contact adsorption method.

The adsorption kinetics experiments were carried out to establish the influence of several parameters (contact time, temperature and initial dye concentration) under mechanical stirring with an initial concentration of 25 $mg.L^{-1}$ of dye and 60 $mg.L^{-1}$ of CESS. The samples were drawn at suitable time intervals from the magnetic stirrer and then filtered. The remaining concentration in the supernatant solution was analyzed using a UV-Vis spectrophotometer (BioMate 6, England) by monitoring the absorbance changes.

The elemental analysis was performed using a Panalytical analyzer (Netherlands). Scanning electron microscopy (SEM) was performed using a FEI Quanta 200 instrument (USA). Infrared (IR) spectra was

obtained with KBr pellets in the range of 4000–450cm-1, using a FT/IR-Vertex 70 spectrometer (Germany). DRX analysis in the solid phase was performed using a X'Pert Pro MPD Panalytical (Netherlands) with Cu anode as the source of X-rays at wavelength λ=1.54 Å. The specific surface area was measured by the BET method using a Pore Size using a Micromeritics ASAP 2020 apparatus (USA).
The amount of dye adsorbed was calculated using the following equation:

$$q_e = \frac{(C_0 - C_e)V}{m} \quad (1)$$

where q_e is the amount adsorbed per gram of adsorbent ($mg.g^{-1}$), C_0 and C_e the initial and equilibrium concentration of dye ($mg.L^{-1}$) respectively. V is the volume solution of dye (L) and m is the adsorbent dosage (g).

3. Results and Discussion

3.2. Characterization of CESS biosorbent

The elemental analysis of CESS showed a high yield of Ca (49.5%) and O (41.4%) compared to small amounts of C (7.79%), Mg (0.39%), Al (0.16%), Sr (0.14%), Si (0.13%) and S (0.11%). The X-ray diffraction analysis of CESS confirmed the presence of portlandite, syn and calcite (Figure 2).

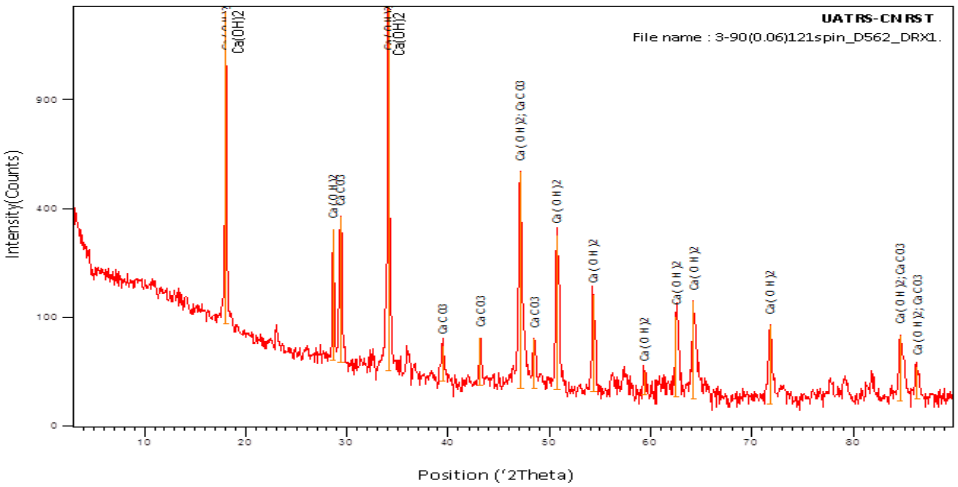

Figure 2: X-ray diffraction of CESS

FTIR analysis was performed in the range of 400–3800 cm^{-1} with resolution 4 (20 scans) in order to explore the surface characteristics of the adsorbent. Figure 3 shows the FTIR spectrum of CESS. The peak positions showing major adsorption bands were observed at 3643, 1442 and 1125 cm^{-1}. The band at 3643 cm^{-1} is due to stretch vibration O-H, the band at 1442 may represent C=C aromatic stretch vibration, and the band at 1125 cm^{-1} represents C–O stretch vibration. In addition to the phosphate bands, the IR analysis also showed bands located between 700 and 880 cm^{-1}, which may be due to the vibration of silicate groups.

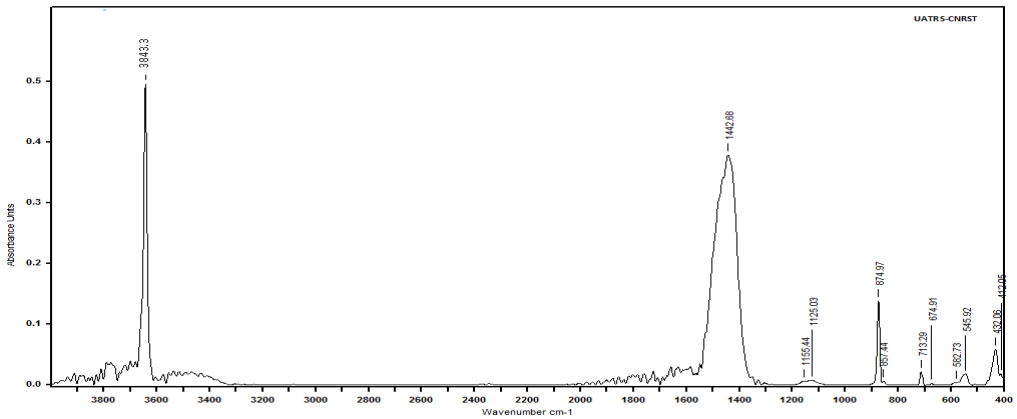

Figure 3: FT-IR analysis of CESS

Scanning electron microscopy has been widely used to study the morphological features of biosorbents. The SEM micrograph of CESS shown in Figure 4 indicated that the biosorbent has a wide distribution of grains of different sizes. The specific surface area of the CESS calculated by the BET method (Brunauer-Emmett-Teller) is 7 $m^2.g^{-1}$.

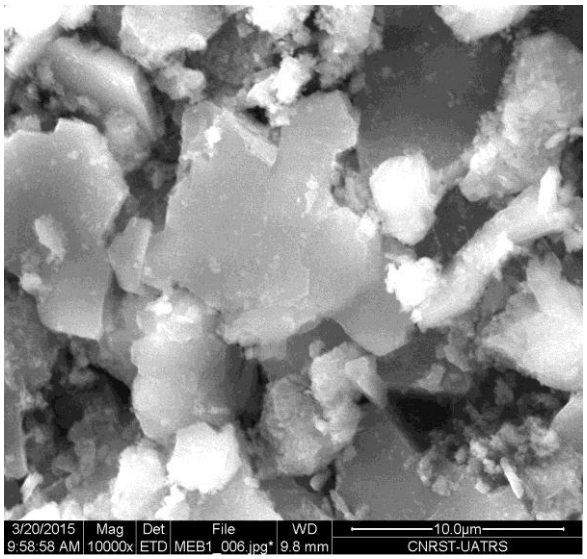

Figure 4: SEM micrograph of the CESS powder treated at 400°C

3.2. Point of zero charge

The pH point of zero charge (pH_{pzc}) of CESS was determined by the salt addition method as described by Chun *et al.* [27] and Muhammad *et al.* [28]. A weight of 100 mg of the sample was added to 95 mL of 0.01 M sodium chloride (NaCl) solution. The pH of the suspension was adjusted to 3-13 by adding HCl (1 N) or NaOH (1 N). The mixture was then kept in an end-to-end water shaker bath for 6 h at ambient temperature. The final pH value of each suspension was recorded after 6 h of equilibration by using a CRISON Ph Meter Basic 20+ (Spain). The PZC of the sample was calculated by plotting ΔpH (final pH–initial pH) versus pH initial (initial pH value). The value obtained at the intersection of the initial pH_i with the ΔpH in Figure 5 gives the pHpzc of the suspended solid, which was found to be around 10.6.

3.3. Effect of adsorbent dosage

Adsorbent dosage is an important parameter because this factor determines the adsorption capacity of an adsorbent for a given initial concentration of the adsorbate [29].

The effect of the dose of calcined *Ensis siliqua* shells was studied by varying the dose between 60 $mg.L^{-1}$ and 120 $mg.L^{-1}$ in aqueous solution of Disperse Red 60 (DR_{60}) and Direct Blue (DB_{71}) dyes. These tests were conducted at a temperature of 25°C and 120 min of contact time to ensure that adsorption was reached.

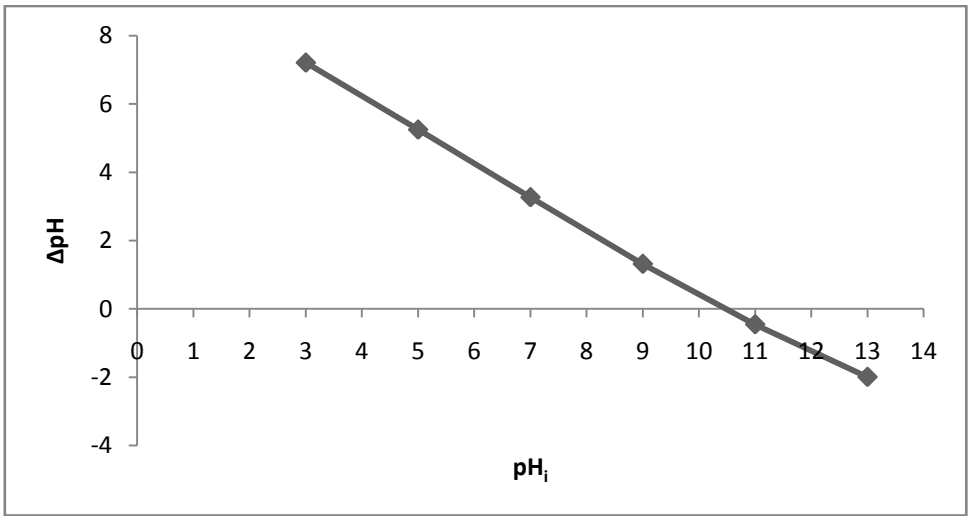

Figure 5: Determination of pH_{pzc} of the CESS

The initial concentration of DR_{60} and DB_{71} was 25 mg.L^{-1}. The removal efficiency of the dyes onto the CESS increased with the increase in biosorbent dose (Figure 6). When the adsorbent concentration was increased from 60 mg to 120 mg, the removal percentage of DR_{60} and DB_{71} increased from 84.18% to 90.40% and from 92.23% to 97.42% respectively, due to the availability of more binding sites as the dose of biosorbent increased.

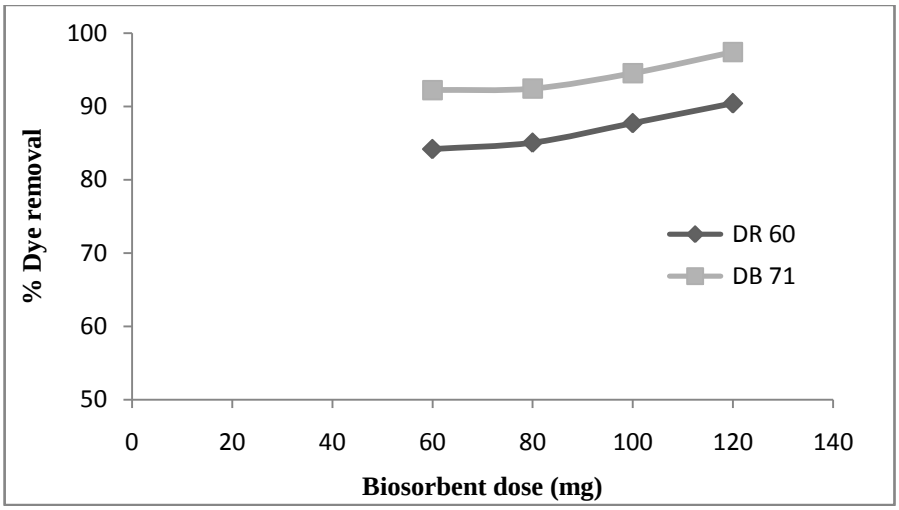

Figure 6: Effect of biosorbent dose on the adsorption of DR_{60} and DB_{71} by CESS

3.4. Effect of contact time and initial dye concentration on the adsorption

The effect of contact time on the percentage removal of the DR_{60} and DB_{71} dyes was investigated at initial dye concentration ranging from 25 to 50 mg.L^{-1}. For both dyes at ambient temperature using 60 mg of biosorbent and with a contact time of 300 min (Figure 7).

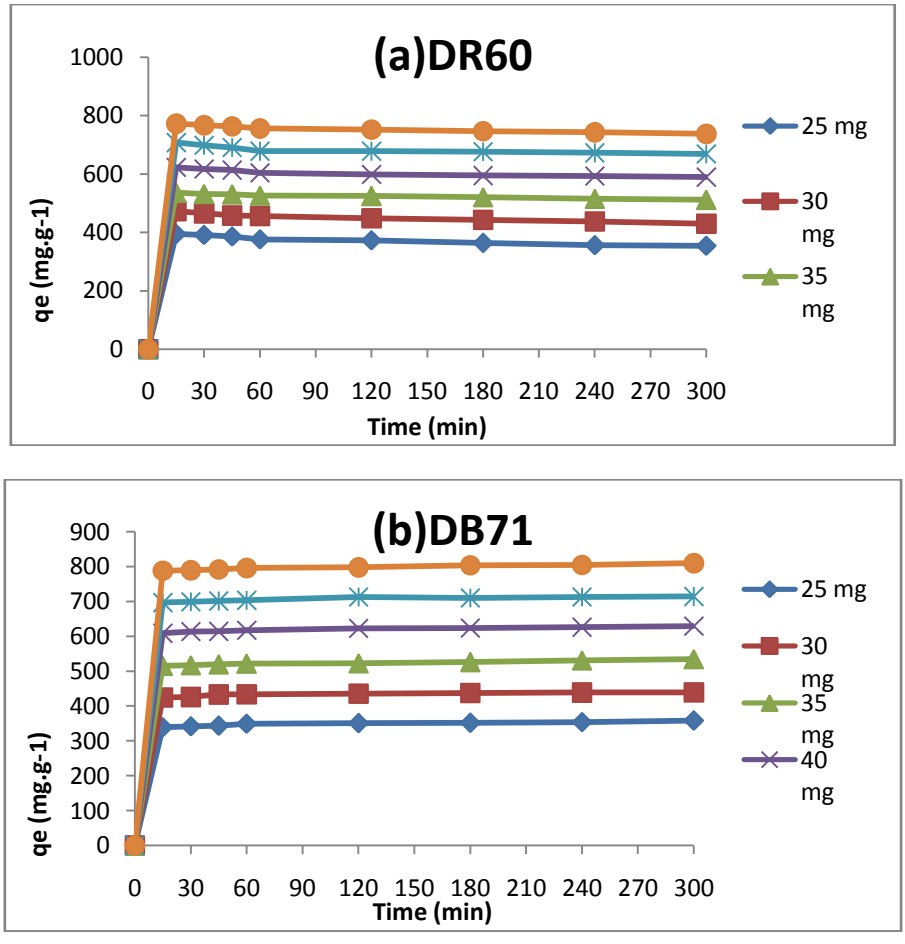

Figure 7: Effect the adsorption time of DR_{60} (a) and DB_{71} (b) by CESS

The amount of dye adsorbed ($mg.g^{-1}$) increased with the increase in contact time. And the amount of dye removed at equilibrium increased from 392 to 752 $mg.g^{-1}$ and from 350 to 797 $mg.g^{-1}$ for DR_{60} and DB_{71} respectively with the increase in dye concentration from 25 to 50 $mg.L^{-1}$. It is clear that the removal of dye depends on the concentration of the dye. The removal efficiency of DR_{60} and DB_{71} onto CESS by adsorption was rapid in the first 15 min due to the larger surface area of adsorbent available, then slowly reached equilibrium after 40 min and remained constant after that. This is because a higher initial concentration provides an important driving force to overcome resistance of the dye between the aqueous and solid phases, thus increasing the uptake. In addition, increasing the initial dye concentration increases the number of collisions between dye ions and the surface area of CESS, which enhances the adsorption process [19].

3.5. Effect of pH

The pH of the dye solution plays an important role in the whole adsorption process and particularly in the adsorption capacity [30]. The effect of pH on adsorption was studied at different pH values (3, 5, 7, 11 and 12). Adjustments were made using 1M HCl or NaOH solution at an initial dye concentration of 25 $mg.L^{-1}$ at 20°C and were the same as those used in the batch adsorption experiments. Samples were intermittently taken in order to measure the amount of dye retained in solution. The effect of pH on the removal of the Disperse Red dye and the Direct Blue dye onto CESS is shown in Figure 8. For DR_{60} the minimum amount of adsorption (about 150 $mg.g^{-1}$) was achieved at pH 3. As the pH was increased from 3.0 to 12.0 the adsorption increased to 332 $mg.g^{-1}$. The dye adsorbed by CESS was higher at higher pH, i.e. with a highly basic solution. Thus the optimum pH adopted for further studies was 12 for DR_{60}. For DB_{71}, the maximum amount of adsorption was about 387.50 $mg.g^{-1}$ at pH 3 and uptake decreased slightly when pH increased from 3.0 to 12.0, so the optimum pH adopted for DB_{71} was 3.0. The results show that basic pH was favorable for the adsorption of DR_{60}, because the negative charge dominates the surface of the adsorbent. Thus, a significantly high electrostatic attraction exists between the negatively charged surface of the adsorbent and positively charged dye species [31]. This attractive force increases the chances of dye species being adsorbed onto the surface of the adsorbent [32]. Up to a pH of 10.6, for DR_{60}, attractive forces increase the adsorption capacity of the material which has a negative charge, whereas for DB_{71} which has more negative charges than DR_{60}, repulsive forces decrease the adsorption capacity of the material. The low aqueous solubility of disperse dyes as reported by Ramakrishna and Viraraghavan [33] will result in a higher affinity for solid surfaces than for water. Disperse dyes are hydrophobic and therefore have a tendency to accumulate at the surface of adsorbents [34]. Thus, the adsorption capacity will increase if the solubility of the dyes is low.

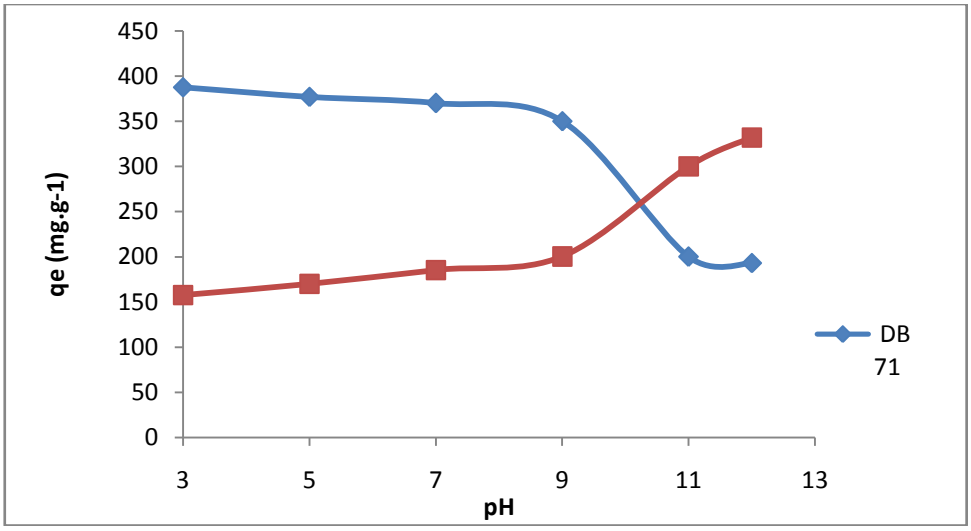

Figure 8: Effect of pH on the adsorption of DR_{60} and DB_{71} by CESS

Concerning DB_{71}, an acidic pH plays a very important role in dye adsorption on CESS. At pH 3, there is a significantly high electrostatic attraction between the positively charged surfaces of the adsorbent, due to the ionization of functional groups of the adsorbent, and the negatively charged anionic dye [25]. When the pH is increased, the electrostatic repulsion increases and the adsorption rate decreases [35]. The lower adsorption of DB_{71} dye at alkaline pH is due to the presence of excess -OH ions destabilizing anionic dyes and competing with the dye anions for the adsorption sites [25].

3.6. Effect of temperature

To determine the effect of temperature on the adsorption of DR_{60} and DB_{71}, experiments were conducted at 20, 30, 40 and 50°C (Figure 9). The equilibrium adsorption capacity of DR_{60} and DB_{71} dyes onto CESS increased with increasing temperature from 20°C to 50°C, indicating that adsorption onto the CESS surface was favored at higher temperatures and that it is controlled by an endothermic process [36].

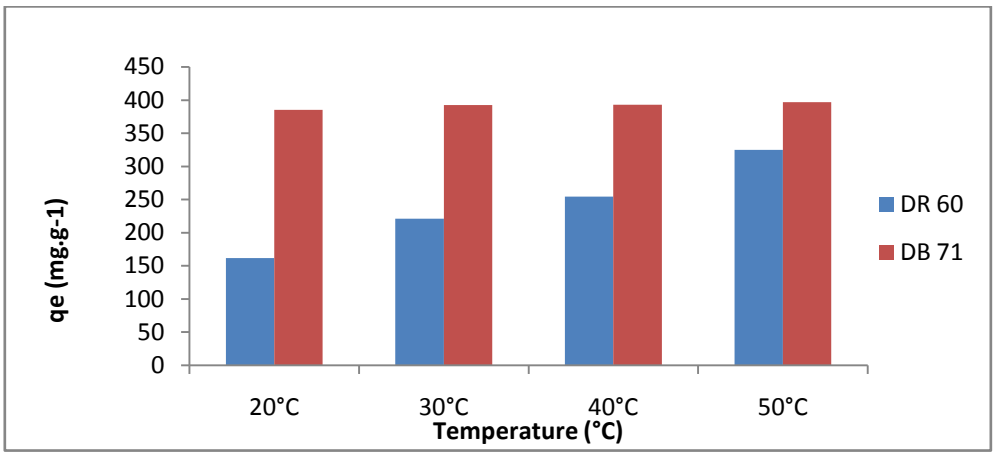

Figure 9: Effect of temperature on the adsorption of DR_{60} and DB_{71}

Concerning DR_{60}, the increase in surface coverage with increasing temperature can be explained by the endothermic spontaneity of the adsorption process. This adsorption is due to electrostatic interactions between the DR_{60} dye and CESS surface at higher temperatures [37].

3.7. Biosorption kinetics

The kinetic behavior of DR_{60} and BD_{71} adsorption was examined using several models. Kinetic models play an important role in determining the biosorption kinetic rates and controlling mechanisms of the adsorption process such as mass transfer and chemical reaction [38]. In order to investigate the adsorption mechanism, characteristic adsorption rate constants were determined using a pseudo first-order Lagergren equation based on solid capacity and a pseudo second-order equation based on solid phase adsorption [39-41]. The integrated form of the pseudo-first-order model is:

$$\ln (q_e - q_t) = \ln (q_e) - k_1 t \qquad (2)$$

where q_e and q_t refer to the amount of dye adsorbed ($mg.g^{-1}$) at equilibrium, respectively, k_1 is the first-order rate constant (min^{-1}) and t is time (min). Values of the rate constant (k_1), equilibrium adsorption capacity ($q_{e,cal}$), and correlation coefficient (R^2) were calculated from the plots of $\ln(q_e - q_t)$ versus t (Figure 10).

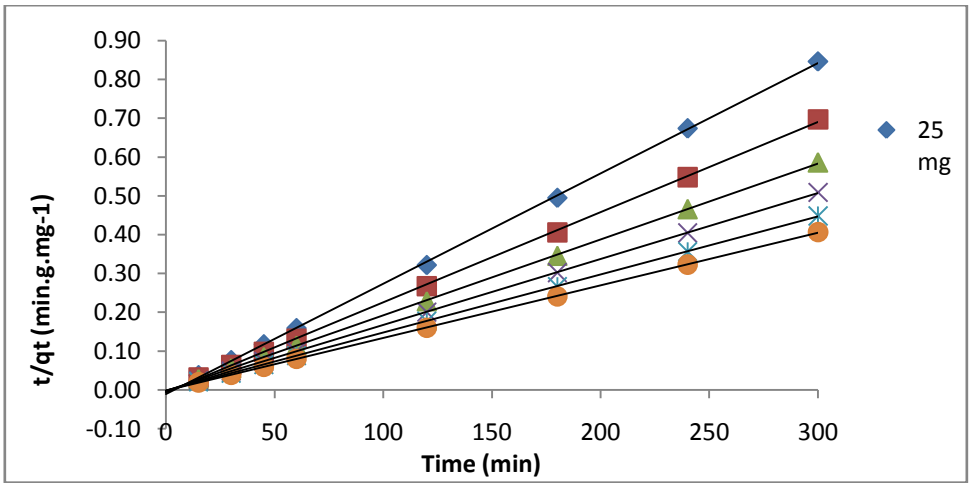

Figure 10: Pseudo-second order kinetic plots for removal of DR_{60} by CESS at different initial dye concentrations

The calculated equilibrium adsorption capacity $q_{e,cal}$ and $q_{e,exp}$ values are presented in Table 1, From Table 1, the lower values of R^2 and the difference between the experimental and calculated equilibrium adsorption show that the pseudo-first-order model failed to describe the adsorption kinetics of the DR_{60} and DB_{71} dyes onto CESS.
If the adsorption does not follow the first-order kinetics, it may also be described by a pseudo-second order kinetic model [42]. The linearized form of the pseudo-second-order model is:

$$\frac{t}{q_t} = \frac{1}{K_2\, qe^2} + \frac{1}{qe}\, t \qquad (3)$$

where k_2 is the value of the rate constant ($g.mg^{-1}min^{-1}$), $q_{e,cal}$ is the equilibrium adsorption capacity, (R^2) the correlation coefficient calculated from the slope and intercept of the plots of t/q_t against t as shown in Figure 10 for DR_{60} and Figure 11 for DB_{71}. The results are presented in Table 1.
From Table 1, the higher values of $R^2 > 0.99$ and the good agreement between the experimental and calculated equilibrium sorption for the pseudo-second-order model confirm that this one describes correctly the biosorption kinetics.

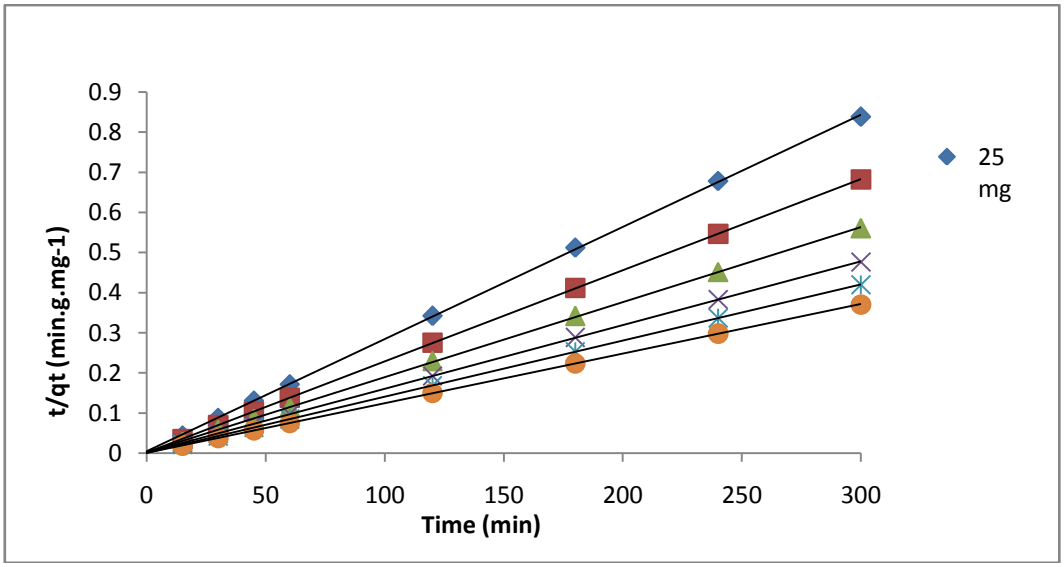

Figure 11: Pseudo-second-order kinetic plots for removal of DB_{71} by CESS at different initial dye concentrations

Table 1: Kinetic constants for dye adsorption onto CESS

			Pseudo-first-order model			Pseudo-second-order		
	Concentration ($mg.L^{-1}$)	$q_{e,exp}$ ($mg.g^{-1}$)	k_1 (min^{-1})	$q_{e,cal}$ ($mg.g^{-1}$)	R^2	k_2 ($g.mg^{-1}.min^{-1}$)	$q_{e,cal}$ ($mg.mg^{-1}$)	R^2
DR_{60}	25	372.96	$7.1x10^{-3}$	6.85	0.715	$0.73x10^{-3}$	357.14	0.9997
	30	448.88	$5.5x10^{-3}$	9.28	0.818	$0.75x10^{-3}$	434.78	0.9997
	35	524.81	$6.8x10^{-3}$	3.68	0.857	$1.21x10^{-3}$	500.00	0.9999
	40	598.88	$5.8x10^{-3}$	7.52	0.678	$1.07x10^{-3}$	588.24	0.9998
	45	678.51	$3.8x10^{-3}$	14.56	0.584	$1.13x10^{-3}$	666.67	0.9996
	50	752.59	$5.3x10^{-3}$	9.84	0.405	$1.15x10^{-3}$	714.29	0.9997
DB_{71}	25	350.64	$74.8x10^{-3}$	124.43	0.799	$1.63x10^{-3}$	384.62	0.9997
	30	435.58	$85.1x10^{-3}$	144.22	0.831	$2.52x10^{-3}$	476.19	0.9993
	35	522.92	$91.8x10^{-3}$	139.08	0.801	$1.06x10^{-3}$	526.32	0.9998
	40	623.08	$66.1x10^{-3}$	153.86	0.667	$1.51x10^{-3}$	625.00	0.9999
	45	712.82	$59.8x10^{-3}$	167.48	0.605	$1.78x10^{-3}$	666.67	0.9999
	50	797.76	$86.4x10^{-3}$	187.97	0.752	$1.31x10^{-3}$	769.23	0.9992

3.8. Biosorption isotherms

The adsorption isotherm indicates how the molecules distribute between the liquid and solid phases when the adsorption process reaches equilibrium. It is important in describing how solutes interact with adsorbents, and is critical in optimizing the use of adsorbents [43]. Analysis of the isotherm data by fitting them to different isotherm models is an important step in finding the suitable model that can be used for design purposes [44]. Four isotherm models were tested to describe the equilibrium adsorption: the Langmuir model [45], the Freundlich model [46], the Dubinin-Radushkevich model (D-R) [47] and the Temkin model [48].

The Langmuir adsorption isotherm has been successfully applied to many sorption processes of monolayer adsorption. The model depends on the assumption that intermolecular forces decrease rapidly with distance and consequently predicts the existence of monolayer coverage of the adsorbate at the outer surface of the adsorbent [49]. The Freundlich equation is an empirical equation employed to describe heterogeneous systems and reversible adsorption and is not restricted to the formation of a monolayer [50]. The Dubinin–Radushkevich isotherm is generally applied to express the adsorption mechanism with a Gaussian energy distribution onto a heterogeneous surface. It distinguishes between physical and chemical adsorptions [51]. Lastly, the Temkin isotherm model assumes that the heat of adsorption of all the molecules in the layer decreases linearly with coverage due to adsorbent–adsorbate interactions and that adsorption is characterized by a uniform distribution of binding energies, up to some maximum binding energy [52]. The equations and linearized form of these isotherm models are given in Table 2.

Table 2: Isotherm models tested in this study

Isotherm	Non linear form	Linear form	plot
Langmuir			
Freundlich	$q_e=K_F C_e^{\ n}$	$\log(q_e)=\log(K_F)+n\log(C_e)$	$\log(q_e)$ vs. $\log(C_e)$
Temkin		$q_e=B_T \ln K_T + B_T \ln C_e$ (with $B_T = \frac{q_m RT}{\Delta Q}$)	q_e vs. $\ln C_e$
Dubinin-Radushkevitch (D-R)	$q_e = q_m \exp(-\beta\varepsilon^2)$ (with $\varepsilon = RT\ln(1+\frac{1}{q_e})$)	$\ln(q_e)=\ln(q_m) - \beta\varepsilon^2$	$\ln(q_e)$ vs ε^2

where:

q_e: Equilibrium sorbate concentration in the solid phase ($mg.g^{-1}$),

q_m: Maximum monolayer adsorption capacity in the multilayer isotherm model ($mg.g^{-1}$),

C_e: Equilibrium adsorbate concentration in the liquid phase ($mg.dm^{-3}$),

K_L: Langmuir isotherm constant ($dm^3.g^{-1}$),

K_F: Freundlich isotherm constant ($dm^3.g^{-1}$),

B_T = Temkin constant which is related to the heat of sorption ($J.mol^{-1}$),

β = D-R isotherm constant ($mol^2.kJ^{-2}$).

R= Gas constant; 8.314 ($J.mol^{-1}.K^{-1}$)

T = Temperature in Kelvin.

The experimental equilibrium data of DR_{60} and DB_{71} onto CESS were compared with the theoretical equilibrium data obtained from the Langmuir, Freundlich, Temkin and D-R isotherm models (Table 3).

The Langmuir, Temkin and Dubinin–Radushkevich models gave a poor fit (Table 3), so are clearly not appropriate for describing the adsorption of DR_{60} and DB_{71} onto CESS, while the Freundlich isotherm model shows a good regression coefficient.

Therefore, the Freundlich equation better represents the adsorption process of DR_{60} and DB_{71} onto CESS which proves that the adsorption surface is heterogeneous with sites which have different adsorption energies.

3.9. Thermodynamic studies

Thermodynamic parameters such as change in free energy ($\Delta G°$) enthalpy ($\Delta H°$) and entropy ($\Delta S°$) were determined using the following equations [53].

$$\Delta G° = -RT \ln K_c \quad (4)$$

where R is the universal gas constant (8.314 $J.mol^{-1}.K^{-1}$), T is the temperature (K) and K_C is the distribution coefficient for adsorption. The K_C value was calculated using the following equation [54]:

$$K_C = \frac{C_e}{q_e} \quad (5)$$

Where K_c is the equilibrium constant, C_e is the solid phase concentration at equilibrium ($mg.L^{-1}$) and q_e is the liquid phase concentration at equilibrium ($mg.L^{-1}$).

Table 3: Isotherm constants for DR_{60} and DB_{71} adsorption onto CESS

	Isotherm model	Parameters		
DR_{60}	Langmuir	----	---	----
	Freundlich	K_F=123.47 $mg^{1-n}.L^n.g^{-1}$	n=1.148	**R^2=0.993**
	Temkin	K_T= 0.6789 $L.mg^{-1}$	B_T=619.1	R^2=0.981
	D-R	q_m=1021.472 $mg.g^{-1}$	β=2 10^{+6}	R^2=0973
DB_{71}	Langmuir	----	---	----
	Freundlich	K_F= 9.403 $mg^{1-n}.L^n.g^{-1}$	n=1.133	**R^2=0.955**
	Temkin	K_T=0.908 $L.mg^{-1}$	B_T=577.7	R^2=0.929
	D-R	q_m=1036.909 $mg.g^{-1}$	β=2 10^{-6}	R^2=0.938

The enthalpy ΔH° and the entropy ΔS° of adsorption were estimated from the following equation:

$$\Delta G° = \Delta H° - T\Delta S° \quad (6)$$

The combination of Equations (5) and (6) gives:

$$\ln K_C = \frac{\Delta S°}{R} - \frac{\Delta H°}{RT} \quad (7)$$

Table 4: Thermodynamic parameters for adsorption of DR_{60} and DB_{71} on CESS

	T (K)	**$\Delta G°$ ($kJ.mol^{-1}$)**	**$\Delta H°$ ($kJ.mol^{-1}$)**	**$\Delta S°$ ($J.mol^{-1}.K^{-1}$)**
DR_{60}	293	-5.75	43	165.95
	303	-7.40		
	313	-8.50		
	323	-10.95		
DB_{71}	293	-12.95	12.36	86.63
	303	-14.10		
	313	-14.65		
	323	-15.65		

The thermodynamic parameters of ΔH° and ΔS° for the two dyes were obtained from the slope and intercept of the plot between LnKC versus 1/T respectively (Table 4). The ΔG° values were negative, suggesting that the adsorption process was favorable and spontaneous in nature. The positive value of ΔH° confirmed the endothermic nature of the adsorption process, which may explain the fact that the adsorption capacity was enhanced by increasing the temperature, while the positive value of ΔS° indicated the increasing randomness at the solid/liquid interface during the adsorption of DR60 and DB71 onto CESS.

Conclusions

The present study shows that the calcined *Ensis siliqua* shells (CESS) prepared from low-cost material are efficient in removing Disperse Red dye 60 (DR_{60}) and Direct blue dye 71 (DB_{71}) from aqueous solution. The adsorption is highly dependent on contact time, adsorbent dosage, and initial concentration. The kinetics of adsorption of the two dyes onto CESS followed the pseudo second-order model.
Analysis of the equilibrium data showed that DB_{71} and DR_{60} followed the Freundlich isotherm model.
The thermodynamic parameters indicated that the adsorption of dyes was feasible, endothermic, and spontaneous in nature. CESS which is an inexpensive and easily available material can be successfully used for the removal of dyes from aqueous solutions and can be an alternative to more costly adsorbents used for dye removal in wastewater treatment processes.

References

1. El Haddad M., Regti A., Laamari M.R., Slimani R., Mamouni R., El Antri S., Lazar S., *J. Taiwan Inst. Chem. Eng.* 45 (2014) 533.
2. Tsui L.S., Roy W.R., Cole M.A., *Color. Technol*. 119 (2003) 14.
3. Salem I.A., El Maazawi M., *Chemosphere* 41 (2000) 1173.
4. Stephenson R.J., Sheldon J.B., *Water Res*. 30 (1996) 781.
5. Rao N.N., Somasekhar K.M., Kaul S.N., Szpyrkowicz L., *J. Chem. Technol. Biotechnol*. 76 (2001) 1124.
6. Szygu1a A., Guibal E., Palacın M.A., Ruiz M., Sastre A.M., *J. Environ. Manage.* 90 (2009) 2979.
7. Karatas M., Argun Y.A., Argun M.E., *J. Ind. Eng. Chem*. 18 (2012) 1058.
8. Moussavi G., Mahmoudi M., *Chem. Eng. J*. 152 (2009) 1.
9. DeLara E.A., Damas S.B., Miranda M.I.A., Clar M.I.I., *J. Hazard. Mater.* 209-210 (2012) 492.
10. Essadki A.H., Bennajah M., Gourich B., Vial C.H., Azzi M., Delmas H., *Chem. Eng. Process*. 47(2008) 1211.
11. Wang A., Qu J., Liu H., Ge J., *Chemosphere* 55 (2004) 1189.
12. Koparal A.S., Yavuz Y., Gurel C., Ogutveren U.B., *J. Hazard. Mater*. 145 (2007) 100.
13. Liua C.H., Wua J.S., Chiua H.C., Suena S.Y., Chub K.H., *Water Res.* 41 (2007) 1491.
14. Paul J., Rawat K.P., Sarma KS.S., Sabharwal S., *Appl. Radiat. Isot.* 69 (2011) 982.
15. Lee Y.C., Kim E.J., Yang J.W., Shin H..J., *J. Hazard. Mater.* 192 (2011) 62.
16. Sudarjanto G., Lehmann B.K., Keller J., *J. Hazard. Mater.* B138 (2006) 160.
17. Robinson T., Chandran B., Nigam P., *Water Res.* 36 (2002) 2824.
18. Meshko V., Markovska L., Mincheva M., Rodrigues A.E., *Water Res*. 35 (2001) 3357.
19. (a) Slimani R., El Ouahabi I., Abidi F., El Haddad M., Regti A., Laamari M.R., El Antri S., Lazar S., *J. Taiwan Inst. Chem. Eng.* 45 (2014) 1578. (b) Riadi Y., Slimani R., Haboub A., El Antri S., Safi M., Lazar S., *Mor. J. Chem*. 1 (2013) 24.
20. Bulut Y., Gözübenli N., Aydın H., *J. Hazard. Mater*. 144 (2007) 300.
21. (a) El Haddad M., Slimani R., Mamouni R., El Antri S., Lazar S., *J. Assoc. Arab Univ. Basic Appl. Sci.* 14 (2013) 51. (b) El Haddad M., Mamouni R., Slimani R., Saffaj N., Ridaoui M., El Antri S., Lazar S., *J. Mater. Environ. Sci*. 3 (2012) 1019. (c) Slimani R., Anouzla A., Abrouki Y., Ramli Y., El Antri S., Mamouni R., Lazar S., El Haddad M., *J. Mater. Environ. Sci.* 2 (2011) 77.
22. (a) Slimani R., El Ouahabi I., Hachoumi I., Riadi Y., Anouzla A., El Haddad M., El Antri S., Lazar S., *Int. J. Environ. Monit. Anal.* 2 (2014) 48. (b) Harkati S., Hamlich M., Echabbi F., Riadi Y., Slimani R., Halim K., Lazar S., Safi M., *J. Mar. Chim. Heterocycl.* 15 (2016) 32.
23. Ardejani F.D., Badii Kh., Limaee N.Y., Shafaei S.Z., Mirhabibi A.R., *J. Hazard. Mater.* 151 (2008) 730.
24. Peláez-Cid A.A., Velázquez-Ugalde I., Herrera-González A.M., García-Serrano J., *J. Environ. Manage*. 130 (2013) 90.
25. Arami M., Limaee N.Y., Mahmoodia N.M., Tabrizi N.S., *J. Hazard. Mater.* 135 (2006) 171.
26. El Nemr A., Abdelwahab O., El Sikaily A., Khaled A., *J. Hazard. Mater*. 161 (2009) 102.
27. Chun H., Yizhong W., Hongxiao T., *Chemosphere* 41 (2000) 1205.
28. Muhammad S., Hussain S.T., Waseem M., Naeem A., Hussain J., Jan M.T., *Iran. J. Sci. Technol.* A4 (2012) 481.

29. Bulut Y., Aydın H., *Desalination* 194 (2006) 259.
30. Wang S., Boyjoo Y., Choueib A., *Chemosphere* 60 (2005) 1401.
31. Namasivayam C., Kavitha D., *Dyes. Pigments*. 54 (2002) 47.
32. Isa M.H., Lang L.S., Asaari A.H.F., Hamidi A.A., Ramli N.A., Jaya Paul A.D., *Dyes Pigments* 74 (2007) 446.
33. Ramakrishna K.R., Viraraghavan T., *Waste. Manage*. 17 (1997) 483.
34. Ozacar M., Sengil A.I., *J. Hazard. Mater*. 98 (2003) 211.
35. Palanisamy, P.N., Raffiea Baseri, J., Sivakumar, P., *E-J. Chem*. 9 (2012) 1122.
36. Bhatnagar A., Jain A.K., *J. Colloid Interface Sci.* 281 (2005) 49.
37. Al Degs Y.S., El Barghouthi M.I., El Sheikh A.H., Walker G.M., *Dyes Pigments* 77 (2008) 16.
38. Vijayaraghavan K., Winnie H.Y.N., Balasubramanian R., *Desalination* 266 (2011) 195.
39. Arami M., Limaee N.Y., Mahmoodi N.M., Tabrizi N.S., *J. Hazard. Mater.* 135 (2006) 171.
40. Namasivayam C., Sumithra S., *J. Environ. Manage*.74 (2005) 207.
41. Allen S.J., Gan Q., Matthews R., Johnson P.A., *J. Colloid Interface Sci*. 286 (2005) 101.
42. Ho Y.S., McKay G., *Process. Biochem.* 34 (1999) 451.
43. Tan I.A., Ahmad A.L., Hameed B.H., *J. Hazard. Mater*.154 (2008) 337.
44. Demiral H., Demiral İ., Karabacakoğlu B., Tümsek F., *J. Int. Environ. Appl. Sci.* 3 (2008) 381.
45. Langmuir I., *J. Am. Chem. Soc.* 40 (1918) 1361.
46. Freundlich H.M.F., *J. Phys. Chem*. 57 (1906) 385.
47. Dubinin M.M., *Chem. Rev.* 60 (2) (1960) 235.
48. Temkin M.I, Pyzhev V., *J. Phy. Chem USSR*. 12 (1940) 327-356
49. El Geundi M.S., Nassar M.M., Farrag T.E., Ahmed M.H., *Alexandria Eng. J*. 51 (2012) 11.
50. Chan L.S., Cheung W.H., McKay G., *Desalination* 218 (2008) 304.
51. Gunay A., Arslankaya E., Tosun I., *J. Hazard. Mater*. 146 (2007) 362.
52. Xiong X.J., Meng X.J., Zheng T.L., *J. Hazard. Mater*. 175 (2010) 241.
53. Gong R., Sun Y., Chen J., Liu H., Yang C., *Dyes Pigments* 67 (2005) 175.
54. Han R., Wang Y., Han P., Shi J., Yang J., Lu Y., *J. Hazard. Mater*. 137 (2006) 550.

(2017) ; http://www.jmaterenvironsci.com